RSC Publishing Faraday Discussions

Magnetophoretic assembly of flexible nanoparticles/lipid microfilaments

Journal:	*Faraday Discussions*
Manuscript ID:	FD-ART-12-2014-000272.R1
Article Type:	Paper
Date Submitted by the Author:	19-Jan-2015
Complete List of Authors:	Bharti, Bhuvnesh; North Carolina State University, Department of Chemical and Biomolecular Engineering Farneau, Anne-Laure; National Institute of French Agricultural Research, Velev, Orlin D; North Carolina State University, Department of Chemical Engineering

CREATED USING THE RSC REPORT TEMPLATE (VER. 3.1) - SEE WWW.RSC.ORG/ELECTRONICFILES FOR DETAILS
Faraday Discussions
PAPER www.rsc.org/faraday_d | Faraday Discussions

Magnetophoretic assembly of flexible nanoparticles/lipid microfilaments

Bhuvnesh Bharti,[a] Anne-Laure Fameau[b] and Orlin D. Velev[a,*]
DOI: 10.1039/b000000x

The directed assembly of colloidal particles into linear chains and clusters is of fundamental and practical importance. In this study we characterize and analyse the mechanism of the magnetic field driven assembly of lipid-coated iron oxide nanoparticles into flexible microfilaments. Recently we showed that nanocapillary lipid binding can form a new class of magnetic nanoparticle-lipid microfilaments with unprecedented flexibility and self-healing properties. In the presence of uniform magnetic field, the magnetophoretic attraction of the particles combined with interparticle dipole-dipole attraction drives the microfilament assembly. The fluid like lipid layer on the particles leads to the surface stickiness of the filaments and the magnetic field concentration overcomes the potential electrostatic repulsion in the water phase. The lipid capillary bridges formed between the particles facilitate their permanent binding and sustain the flexible microfilament structure. We demonstrate that this surface stickiness combined with the filaments' magnetic response can be used further to twist, bend and bundle the microfilaments into unusual structures.

1 Introduction

The development of novel strategies for assembly of nano- and micro-sized building block particles into ordered supracolloidal structures is of fundamental interest, as well as of practical importance in industrial and biological processes.[1-4] The equilibrium assembled state of the colloidal particles is determined by the interparticle interactions, which can be tuned in strength and directionality to obtain one-, two- or three- dimensional assemblies of desired morphology and symmetry.[5-7] These assemblies and their hierarchal organization have been used widely in various industrial applications such as anti-reflective coatings, photonic crystals, tissue scaffolding and sensors.[8,9] Linear chains and filaments from particles form an important class of supracolloidal assemblies, which could be used in applications such as conductive microwires, LEDs, single-electron transistors and artificial flagellum.[10-13]

[a]*Department of Chemical and Biomolecular Engineering, North Carolina State University, Raleigh, NC, USA. E-mail: odvelev@ncsu.edu, Tel: +1-919-513-4318*
[b]*National Institute of French Agricultural Research, Nantes, France*

One of the most effective ways to assemble randomly distributed colloidal particles is the application of external electric and/or magnetic field(s).[8-10,14] The external fields polarize the individual particles and the interparticle dipole-dipole attraction drives their assembly into pearl-necklace type arrangement.[14-16] However, typically the assembled particles retain their configuration only as long as the external field is present and it falls apart into randomly dispersed particles upon switching off the field. The disintegration is most often a result of the interparticle surface charge repulsion and the particles' random thermal motion.

The application of external fields for the directional assembly of nanoparticle chains, filaments and networks is of significant interest, as such structures can find applications in areas such as electronics, functional complex fluids, tissue scaffolding and micro-robotics.[8-12] The common pattern formed by particles in external fields is chains of single particle diameter. The formation of dipolar chains in colloidal systems is the functional basis of magneto- and electro-rheological fluids. There are, however, cases where nanoparticles can be assembled in much thicker filaments. We have earlier demonstrated that metallic nanoparticles can be permanently assembled into microwires by applying external electric field.[10] The analysis of the assembly process showed that it is not dominated by induced dipole-dipole chaining. Rather, the tip of the growing microwire creates an area of high field intensity, which attracts the particles by a gradient-driven dielectrophoretic force.[17] Overall, one can distinguish two physically different mechanisms of assembly of single-particle diameter chain-like and multi-particle diameter fibrillar structures; the former is formed via dipole-dipole attraction and the latter by field-gradient nanoparticle collection.

Interestingly, most studies of magnetic field nanoassembly deal with dipolarly interacting colloids, which form single particle diameter chains.[15] However, dielectrophoretic assembly of thick microfilaments is prevalent in the case of directed assembly of nanoparticles in electrical fields. We are not aware of studies, where thick nanoparticle microfilaments have been assembled by magnetophoretic attraction to the end of an assembling filament. One of the reasons for the paucity of detailed investigations of thick, magnetophoretically assembled, nanoparticle filaments is the practical requirement that the nanoparticles in these chains should be bound together by an interaction potential that is strong enough to keep them together, yet will allow for enough flexibility for the assembled filaments to preserve their integrity when further dragged and rotated in the magnetic field. The most commonly used strategies for permanently binding nanoparticles include surface coating with organic or inorganic molecular layers.[18,19] Such binding schemes generally yield inflexible links between the particles and result in rigid assemblies. Semi-flexible chains of colloidal particles can be obtained by interlinking particle-to-particle junction points with polymeric "colloidal linkers" such as polystyrene, DNA and polyacrylic acid.[20-24] These links provide permanent binding between the particles but they may lack the simplicity, robustness and reconfigurability needed for binding of thicker, disordered nanoparticle microfilaments.

Recently, we reported a novel route to bind magnetic nanoparticles via ultraflexible fluid linkages.[25] We demonstrated that iron (II) oxide nanoparticles can be arrested into contact by fluid capillary bridges. The fluid fatty acid bridging provided an unusual means of particle-to-particle linkage imparting ultrahigh

flexibility and self-healing properties to the assembled structures.[25] We present here data on the dynamics of formation and the properties of thick fibrillar nanoparticle assemblies in magnetic field. We analyse the (magnetophoretic) origins of the process leading to the formation of the thick fibrils and evaluate the field distribution leading to these processes. Two distinct features of the process are outlined and discussed: (1) The nanoparticles migration and assembly in external magnetic field; and (2) The reconfiguration of the structure bound by lipid bridging upon timed switching of the field. We develop a better understanding of the magnetic field driven multiparticle chaining and the factors governing the assembly process, including the role of the capillary bridging forces in making possible the nanoparticle rearrangement. We also briefly discuss the strategies to assemble filaments and their networks into configurations of closed loops and multifilament bundles.

2 Methods

2.1 Experimental details

The experiments were perfomed using 12-hydroxysteric acid (Sigma-Aldrich, purity 75%) and γ-Fe_2O_3 spheroidal particles (~ 20 nm, M K Impex Corp., purity 99 %) as representative lipid and superparamagnetic nanoparticles. A 1 mg/ml fatty acid aqueous solution was prepared by mixing solid 12-hydroxysteric acid pallets with equimolar concentration of ethanolamine as the counter ion.[26] The fatty acid salt solution was then mixed with solid γ-Fe_2O_3 nanoparticles (final concentration = 1 mg/ml). The mixture was first heated to 80 °C and then sonicated for 10 min at room temperature to achieve a better dispersibility of the iron oxide microaggregates in aqueous solution. The assembly of lipid coated magnetic nanoparticle building blocks into microfilaments is driven by a uniform magnetic field applied across the assembly chamber (25 mm × 25 mm × 0.22 mm) using two co-plannar electromagnets powered from a DC source [16 V, 0-5 A]. The dispersion was immediately transferred on to the experimental chamber and a uniform magnetic field (~ 5000 A/m) was applied instantaneously. The field characteristic such as intensity, polarization and gradient were fine-tuned by varying the current flowing through the two coils. The process was monitored using an upright Olympus BX-61 bright field microscope.

2.2 COMSOL™ simulations

The magnetophoretic assembly is guided by the distribution of the external magnetic field. To interpret the assembly mechanism, we perform COMSOL™ numerical simulations and investigate the distribution of local magnetic fields around a microfilament tip. The calculations were done using AC/DC module of COMSOL™ simulation package version 4.2a. For simplicity, the simulations were carried out in two-dimension simulation box of size 500 × 500 nm^2. The lipid-coated particles were approximated with a 20 nm circular magnetic core and a 5 nm non-magnetic lipid shell. The relative permeability (μ) of lipid shell and magnetic core respectively were ~ 1 and 7.[27] The relative magnetic permeability of the aqueous dispersion was approximated to be ~ 1. The computational package discretizes the calculation space by adaptive triangular mesh and solves Maxwell's equations for each mesh domain. The simulations were performed in an iterative manner, and were

continued until the solution converged with < 1 % variation in the relative tolerance value between two consecutive iterations.

3 Assembling lipid coated nanoparticles into filaments

3.1 Magnetic field driven assembly of filaments

External fields are widely used to assemble linear chains of colloidal particles.[28] In this study we assemble lipid coated iron oxide nanoparticles into multiparticle thick filaments. Figure 1a presents a micrograph of the iron oxide nanoparticles and their micro-aggregates dispersed in aqueous fatty acid salt solution (for details see Section 2.1). Recently we showed that the water-soluble fatty acid molecules selectively condense onto iron oxide nanoparticles' surfaces forming a fluid nanoshell and that upon the application of a uniform magnetic field these coated particles assemble into permanent filaments.[25] The microfilament assembly process can be divided into two distinct steps. In the first step, the dispersion is subjected to a uniform magnetic field, resulting into the linear alignment of lipid capped nanoparticles and their aggregates into microfilaments along the direction of applied field (Fig. 1b). In the second step, the external magnetic field is switched off, effectively eliminating the interparticle magnetic attraction. In our previous study on electric field driven assembly of negatively charged particles, we demonstrated that upon switching off the external field, the assembled linear chains disintegrate into their particulate form.[22,29] However in the present case of lipid-coated iron oxide nanoparticles, the assembled filaments retain their configuration by the formation of lipid capillary bridges (Fig. 1d).[25] As shown in Figure 1c, the microfilaments attain undulated relaxed confirmations upon switching off the magnetic field, which can be attributed to the thermal fluctuations and surrounding fluid microflows.

Our previous report showed that the length of assembled microfilaments was governed by the nanoparticle and lipid concentrations, and applied field strength and duration.[25] Here we report data on the kinetics of formation of the microfilaments in external uniform magnetic field. The rate of increase of the mean filament length was determined by microscope image analysis. The obtained variation in the mean filament length and the rate of filament formation during the assembly process in the field ON state are plotted in Fig. 1e. The initial rapid increase in the rate of filament formation can be attributed to the availability of a highly concentrated assembling building blocks, i.e. lipid coated nanoparticles (broadly analogous to polymer reactants). The depletion in the local concentration of unbound free nanoparticles in the vicinity of the microfilaments will lead to a decrease in the rate of filament growth. The mechanism of the filament assembly is examined in the following section.

3.2 Analysis of the filament assembly mechanism

The equilibrium morphology of the assembled microfilaments is dependent on the mechanism of their formation. In order to understand the assembly mechanism we performed a visualization of the filaments' nanoscale structure using scanning and transmission electron microscopy (Fig. 2a and 2b). It should be noted that due to large difference of the electron density between the lipid shells and magnetic nanoparticle cores, the lipid shells remain invisible to the incident electron beam. A

typical scanning electron microscopy image of the filaments in their undulated dried state is shown in Figure 2a. The image illustrates the presence of nano- and microscale irregularities in the filament cross section (Fig. 2a). In addition, the SEM images show a decrease in the cross-section diameter of the filament away from the centre along its contour. This observation is further confirmed by the TEM micrographs (Fig. 2b). The variation of filament width along its contour was quantified by TEM image analysis. As seen from Figure 2c, the filament width is maximal at its centre (~ 3 μm) and decreases monotonically to a single nanoparticle diameter at the filament tips (inset Fig. 2b). The solid line in Figure 2c is the Gaussian fit to the experimental data (squares), where L is the filament length and d is the maximum filament diameter. Within the experimental error, the middle point of the Gaussian fit overlaps with the filament centre.

For understanding the observed filament structure we simulate the magnetic field driven multiparticle assembly process using COMSOL^{TM} simulation package. The details of the simulations are given in Section 2.2. A series of snapshots of simulations of the magnetic field intensity performed for different stages of filament growth along the direction of magnetic field (here horizontal) is shown in Figure 2d-e. As visualized by the high field intensity near the tip of the growing filament, this tip creates a gradient of the magnetic field and directionally attracts the dispersed nanoparticles by magnetophoresis, force driving the polarizable particles along the field gradient. In external magnetic field, this phenomenon of directional attraction of the nanoparticles towards the tips of the filament is primary responsible for collecting the nanoparticles from the surrounding medium and filament growth. In the vicinity of the filament tips, the magnetophoretically driven particle collection will create a local hemispherical region with decreased nanoparticle concentration. The transport of unbound nanoparticles from bulk to the magnetophoretically depleted regions occurs by Brownian diffusion. The depleted region is formed because the rate of magnetophoretic transport of the nanoparticles towards the magnetic filaments is higher than the rate of particle diffusion from bulk. The particle depletion in front of the filaments also explains our data showing decrease in the rate of particle assembly with time (Fig. 1e). We believe that this non-trivial growth mechanism leads to the monotonic increase in the filament diameter from the filament ends towards its centre (Fig. 2c). The decrease in the rate of filament assembly with time can be approximated by an exponential decay with coefficient ~ 0.3 (dotted line in Fig. 1e). Further studies will investigate the exact relation between the decay coefficient and field parameters.

The proposed filament assembly mechanism is broadly similar in its origins to the process of AC electric field driven assembly of gold microwires from nanoparticle suspensions that we reported previously.[10] Once the gold nanoparticles from their aqueous dispersion become concentrated at the filament tip, they rapidly aggregate in a loose thick body, leading to growth of the overall assembled structure. To the best of our knowledge, such mechanism of filament assembly and growth has not been reported for magnetic field driven nanoparticle assembly. We believe it is partially enabled by the strong, yet flexible, binding enabled by the lipid coated nanoparticles snapping into contact. In the following section we briefly discuss these capillary bridging forces that make possible the permanent binding of the nanoparticles into these filamentous assemblies.

3.3 Fundamentals of fluid mediated capillary bridging

The formation of the flexible filaments is enabled by the interparticle capillary bridging forces, which we investigated and quantified in our earlier report.[25] We only present here a brief discussion of these forces and their role in the microfilament assembly. The capillary forces operating between macroscopic surfaces are well-known and extensively studied in literature.[30-32] These forces operate when the particles interact via fluid interfaces and are classified as either normal and lateral.[33] The lateral capillary forces operate between the particles adsorbed at air-liquid or liquid-liquid interfaces and have been used as facile tool to self-assemble electric microcircuits and various types of (millimetre-sized) objects floating on the surface of a liquid.[30,31]

Forces that are directed normal to the plane of contact lines of fluid on the particles are termed as normal capillary forces.[34] The capillary interactions are involved in the flexible linking of the lipid-coated nanoparticles into filaments via liquid bridges. Similar capillary bridging on the microscale offers unconventional ways to assemble particles in bulk on the microscale.[30,31] In many cases, these capillary forces can be larger in magnitude than conventional colloidal forces such as van der Waals and repulsive electrostatic ones.[32] Even a small amount of liquid wetting the particles and immiscible with the continuous phase can induce capillary bridging in microparticle suspensions and may completely change their viscoelastic properties.[35]

The hypothesized pair-interaction-potential operating between fluid coated nanoparticles is schematically presented in Figure 3. As the process uniquely takes place in water medium, the particle and lipid surfaces would be charged and an initial repulsion between the surface condensed fatty acid molecules and weakly bound counter ions would result into a long-range repulsive barrier. The formation of the capillary bridges thus requires some energy to overcome the initial repulsion between the lipid coated particles (Fig. 3). We found that the thermal energy of the particles is barely sufficient to overcome these energy barriers, which will result into slow formation of fractal aggregates via diffusion limited aggregation. In the magnetophoretic assembly, we provide the energy to the lipid coated iron oxide nanoparticles by external magnetic field, which serves dual purpose: (1) It accelerates the capillary aggregation process by providing strong magnetic attraction between the particles; and, (2) It directs the aggregation of the particles into well-defined linear structures. Once the particles are magnetophoretically collected and brought to a distance $r = r_{cap}$, where the lipid shells of two particles overlap each other, the mutual repulsion instantaneously changes to a strong attraction corresponding to the capillary bridge formation. Further decrease in the interparticle separation to r_{ste} induces a strong repulsion between the particles because of the osmotic pressure developed by the hydrocarbon tails of the fatty acid molecules directly bound to the individual iron oxide nanoparticles' surface. The steric repulsion at r_{ste} inhibits the irreversible aggregation of particles into van der Waals global minimum. The proposed interparticle interaction potential curve for fatty acid and iron oxide nanoparticle system is in agreement with recently proposed interaction potential between the propanal coated colloidal silica, where shearing of the medium results into the capillary bridging and aggregation of the particles.[36] It allows for the formation of links that are unique in being strong, reformable and flexible, which is not the usual case with intermolecular and biomolecular binding.

This soft potential also has a number of interesting implications resulting in the unusual magnetic response of the assembled microfilaments as described in more detail below.

4 Hierarchal filament reassembly

The lipid shell on the iron oxide nanoparticles induces a sticky interparticle pair potential (Fig. 3) which upon any instance of shell-to-shell overlap will induce semi-permanent binding. The outer surfaces of the magnetic field formed filaments possess similar binding and stickiness properties. Hence, any direct contact between the surfaces along the filament contours will lead to adhesion or linking, which will persist under normal thermal perturbations. In this section, we show that surface stickiness and flexibility of the microfilaments combined with their instantaneous magnetic response can lead to their buckling into cyclic and bundled structures.[37] We report two types of reconfiguration and reassembly process, self-reassembly and collective multi-filament reassembly.

4.1 Self-reassembly and buckling of filaments in time-switched magnetic field

The capillary bridged filaments remain in their stretched linear configuration in the presence of a uniform unidirectional magnetic field. However, changes in the magnetic field direction result into their spatial reorganization to attain the minimum energy configuration in the altered field. This reorganization typically involves torque components acting on the filaments' contour and twisting the structure. In this section we specifically consider the case of low filament number density, where the individual filament response remains independent of other filaments in its vicinity. In an aqueous dispersion with pre-aligned microfilaments, we reversed the direction (i.e. polarity) of the external magnetic field instantaneously and recorded the dynamics of filament reorganization driven by magnetic torque and polarization forces. The reversal in the field direction initiates in-plane flipping of the filaments. This reorientation can occur only via two intermediate curling pathways (a) cis-pathway; and (b) trans-pathway curling. Cis- and trans- here refer to the intermediate configurations where the two ends of a filament flip from the same and opposite side respectively.[25] The free ends of filaments in cis- and trans-intermediates snap together because of the capillary and/or magnetic interactions and buckle into ring and infinity type loops respectively (Fig. 4a and 4b). As the "sticky" filament ends meet, they snap on contact and upon switching off the external field, the formed loop configurations were retained. We believe that the induced opposite magnetic poles in the ends of a filament drive the dynamics of reconfiguration and snapping. The subsequent semi-permanent binding of the filament contours is due to the sticky nature of the lipid-coated particles on the surface of the structures.[25]

In addition to these two closed structures, a variety of other filament loops were observed. Figure 4c and 4d present two such examples where filaments were reassembled into square and heart shapes. We believe that the deviations in the local bending modulus of the filaments along their contours are responsible for the formation of these unusual loop structures. Based on the light microscopy and SEM micrographs (Fig. 4c. 4d, and 3a), this variation in the bending modulus along the filament contour can be attributed to the incorporation of nanoparticle

microaggregates during the microfilament assembly process. In addition, the equilibrium looped state of the filaments is determined by the length of the filaments and applied magnetic field properties (intensity and frequency). The present report specifically aims at demonstrating the unusual curling behaviour of the microfilaments and is not focused on methodologies to direct the morphology of the looped structures. One possible method of controlling these local moduli of the filaments and hence their equilibrium state is to incorporate micron-sized beads into the microfilaments. Each embedded particle will act as a nodal point and would direct the looping behaviour. However, the curling behaviour of microbead-microfilament composite structures are beyond the focus of present report and would be part of a future publication. As mentioned above these individual shapes are observed in the specific case where the inter-filament interaction and stereorestrictive interactions were absent. In the following section we investigate the implications of high filament density and mutual interactions on the reassembly of filaments in a 2D rotating field.

4.2 Stereorestrictive reassembly of filaments in rotating magnetic fields

In our previous report we demonstrated that by tuning the iron oxide nanoparticle and the lipid concentrations, complex percolated networks of the filaments can be obtained.[25] Micrographs of such 2D percolated network in the absence of any external field are shown in Figure 4e. The filaments in the network are interconnected and are restrained from reorienting upon change in magnetic field polarizibility. These spatial restrictions on the filament reorientation combined with the filament flexibility, stickiness and magneto-responsiveness enable the clustering and bundling of percolated filament networks. Figure 4e-g presents a few examples of such structures via snapshots of the dynamic reconfiguration of the filament network in a 2D rotating magnetic field. The elongated filaments first reconfigure into partially entangled or bent state. At this stage, discrete bundle nuclei begin to form where multiple filaments start curling along one of their ends. We believe that the spatial distribution of the bundles is determined by the local entanglement of the filaments in the network. A prolonged exposure of the network to the rotating magnetic field leads to a complete filament bundling (Fig. 4g). Similar to the filament curling (Section 4.1), the bundling is also initiated by the external magnetic field but the permanent nature of the structure is the implication of fluidity or stickiness of the lipid present on their surface. The bundles present another level of hierarchical organization of the nanoparticles. The bundling and restructuring of the sticky filaments may have broad similarity to, e.g., the formation of hierarchical structures during the gelation of attractive protein microfibrils.[38,39] From practical materials perspective, the magnetic networks with on-demand collapse and/or bundling may allow for precise control over the viscoelastic and transport properties of dispersions and surfaces; and hence may find various industrial and biotechnological applications.

5 Conclusions

We demonstrated that external magnetic field can direct the aggregation of lipid coated sticky iron oxide nanoparticles into unusually thick and flexible microfilaments.[25] We propose a magnetophoretic mechanism of nanoparticle

assembly into filaments and their growth. The COMSOL^{TM} simulations of the magnetic field show that the high field intensity at the two ends of the growing filaments drives the preferential nanoparticle binding at these sites by magnetophoretic attraction. The rate of filament assembly is limited by the depletion of the nanoparticles in the hemispherical regions around the two ends of a growing filament (binding sites). Further we show that by instantaneous change in the field direction, the filaments can be reconfigured into closed loop structures. The combined effect of filament stickiness, local bending rigidities and surrounding fluid viscosity leads to their unusual equilibrium and non-equilibrium configurations. An organization of the nanoparticles on another length-scale can be achieved when the filament network is reconfigured into discrete bundles in a 2D rotating magnetic field. This bundling of filaments in a network was attributed to the combined effect of magnetic field induced actuation, filament stickiness and the stereo-restrictions on the filament rotation.

Acknowledgements

The authors gratefully acknowledge the financial support by NSF Research Triangle MRSEC on Programmable Soft Matter (DMR-1121107). ALF thanks BIA-INRA Nantes for her faculty fellowship. We also acknowledge Dr. Cédric Gaillard (INRA, France) for the TEM imaging.

References

1 Y. Mai and A. Eisenberg, *Chem. Soc. Rev.*, 2012, **41**, 5969.
2 J. C. Huie, *Smart Mater. Struct.*, 2003, **12**, 264.
3 J.-M. Lehn, *Science*, 2002, **295**, 2400.
4 P. Van Rijn, M. Tutus, C. Kathrein, L. Zhu, M. Wessling, U. Schwaneberg, and A. Böker, *Chem. Soc. Rev.*, 2013, **42**, 6578.
5 R. Chakrabarty, P. S. Mukherjee and P. J. Stang, *Chem. Rev.*, 2011, **111**, 6810.
6 G. M.Whitesides and B. Grzybowski, *Science*, 2002, **295**, 2418.
7 B. Bharti, M. Xue, J. Meissner, V. Cristiglio and G. H. Findenegg, *J. Am. Chem. Soc.*, 2012, **134**, 14756.
8 O. D. Velev and S. Gupta, *Adv. Mater.*, 2009, **21**, 1897.
9 F. Bai, D. Wang, Z Huo, W. Chen, L. Liu, X. Liang, C. Chen, X. Wang, Q. Peng and Y. Li, *Angew Chem. Int. Ed.*, 2007, **46**, 6650.
10 K. D. Hermanson, S. O. Lumsdon, J. P. Williams, E. W. Kaler and O D. Velev, *Science,* 2001, **294**, 1082.
11 M. S. Gudiksen, L. J. Lauhon, J. Wang, D. C. Smith, and C. M. Lieber, *Nature*, 2002, **415**, 617.
12 C. Thelander, T. Martensson, M. T. Björk, B. J. Ohlsson, M. W. Larsson, L. R. Wallenberg and L. Samuelson, *Appl. Phys. Lett.*, 2003, **83**, 2052.
13 R. Dreyfus, J. Baudry, M. L. Roper, M. Fermigier, H. A. Stone and J. Bibette, *Nature*, 2005, **437**, 862.
14 S. Gangwal, O. J. Cayre and O. D. Velev, *Langmuir*, 2008, **24**, 13312.
15 a) R. Kretschmer and W. Fritzsche, *Langmuir*, 2004, **20**, 11797. b) M. Wang, L. He, and Y. Yin, *Mater. Today*, 2013, **16**, 110.
16 O. D. Velev and K. H. Bhatt, *Soft Matter,* 2006, **2**, 738.
17 K. H. Bhatt and O. D. Velev, Langmuir, 2004, **20**, 467.
18 W. H. Chong, L. K. Chin, R. L. S. Tan, H. Wang, A. Q. Liu and H. Chen, *Angew. Chem. Int. Ed.*, 2013, **52,** 8570.
19 B. D. Korth, P. Keng, I. Shim, S. E. Bowles, C. Tang, T. Kowalewski, K. W. Nebesny and J. Pyun, *J. Am. Chem. Soc.*, 2006, **128**, 6562.
20 L. J. Hill, and J. Pyun, *ACS Appl. Mater. Interfaces*, 2014, **6,** 6022.

21 M. B. Bannwarth, S. W. Kazer, S. Ulrich, G, Glasser, D. Crespy and K. Landfester, *Angew. Chem. Int. Ed.*, 2013, **52**, 1.
22 B. Bharti, G. H. Findenegg and O. D. Velev, *Langmuir*, 2014, **30**, 6577.
23 D. Li, S. Banon, and S. L. Biswal, *Soft Matter*, 2010, **6,** 4197.
24 L. Cohen-Tannoudji, E. Bertrand, L. Bressy, C. Gaubault, J. Baudry, J. Klein, J.-F. Joanny and J. Bibette, *Phys. Rev. Lett.*, 2005, **94,** 038301.
25 B. Bharti, A.-L. Fameau, M. Rubinstein and O. D. Velev, *under review* 2015, **X**, xx.
26 A.-L. Fameau, S. Lam and O. D. Velev, *Chem. Sci.*, 2013, **4**, 3874.
27 S. Smoukov, S. Gangwal, M. Marquez and O. D. Velev, *Soft Matter*, 2009, **5**, 1285.
28 B. Bharti and O. D. Velev, *Langmuir*, 2015, *in press*
29 B. Bharti, G. H. Findenegg and O. D. Velev, *Sci. Rep.*, 2012, **2**, 1004.
30 D. H. Gracias, J. Tien, T. L. Breen, C. Hsu and G. M. Whitesides, *Science*, 2000, **289**, 1170.
31 T. L. Breen, J. Tien, S. R. J. Oliver, T. Hadzic and G. M. Whitesides, *Science*, 1999, **284**, 948.
32 Y. Min, M. Akbulut, K. Kristiansen, Y. Golan, and J. N. Israelachvili, *Nat. Mater.*, 2008, **7,** 527.
33 P. A. Karlchevsky and N. D. Denkov, *Curr. Opin. Colloid Interface Sci.*, 2001, **6**, 383.
34 H.-J. Butt and M. Kappl, *Adv. Colloid Interface Sci.*, 2009, **146**, 48.
35 E. Koos and N. Willenbacher, *Science*, 2011, **331,** 897.
36 N. Hijnen and P. Clegg, *Langmuir*, 2014, **30**, 5763.
37 A. Cebers, *Curr. Opin. Colloid Interface Sci*, 2005, **10**, 167.
38 T. M. Svitkina, Y. A. Rovensky, A. D. Bershadsky, J. M. Vasilliev, *J. Cell Sci.*, 1995, **108**, 735
39 C. Wang, L. Zhang, M. Yuan, Y. Ge, Y. Liu, J. Fan, Y. Ruan, Z. Cui, S. Tong and S. Zhang, *Plant Biology*, 2010, **12**, 70.

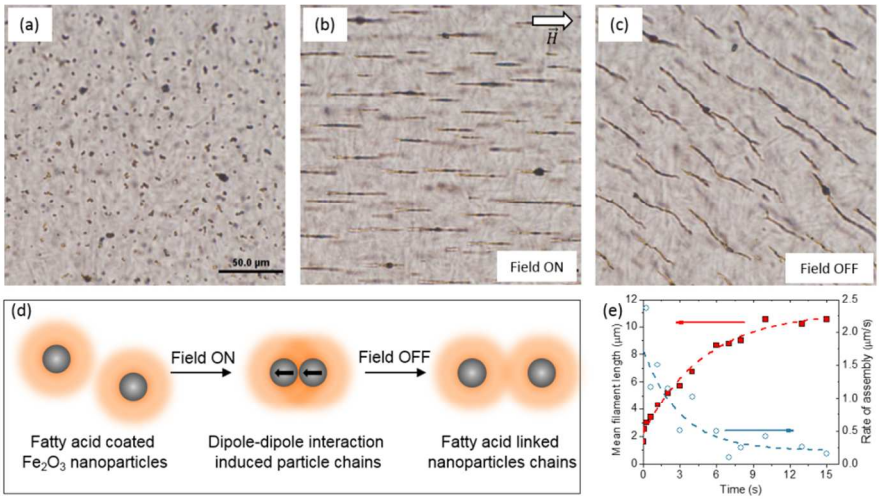

Figure 1. (a-c) Microscope images of 20 nm iron oxide nanoparticles and their aggregates dispersed in the aqueous fatty acid salt solution. (b) The particles align in the direction of applied magnetic field and form linear structures. (c) The linear assemblies attain undulated configuration under surrounding fluid flow but remain assembled in fibrils upon switching off the external magnetic field. (d) A stepwise schematic representation of the magnetic field driven assembly of iron oxide-fatty acid core-shell composite nanoparticles. (e) Kinetics of change of the mean chain length (squares) and rate of filament growth (circles) in the uniform external magnetic field (~ 5000 A/m). The data points are the experimentally obtained mean filament lengths and the dotted lines are the fits using exponential functions.

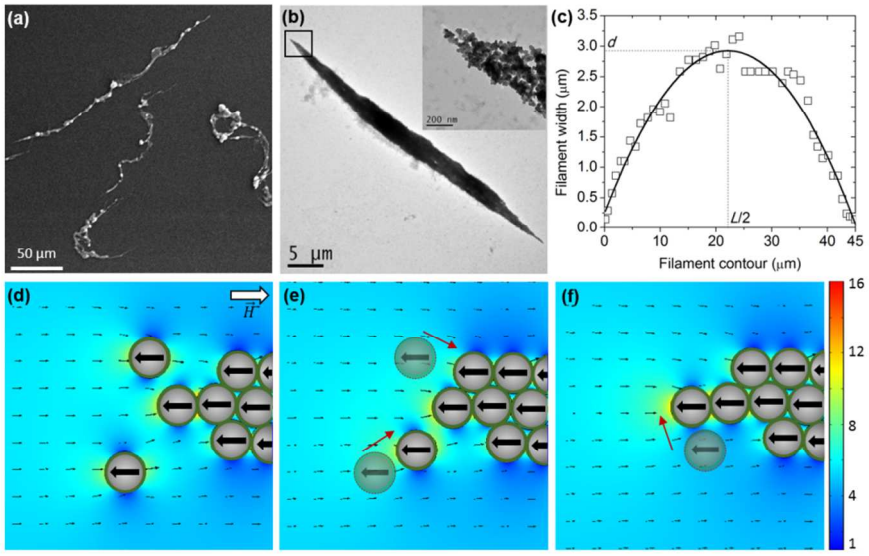

Figure 2. (a) Scanning electron micrograph (SEM) of the iron oxide-nanoparticle filaments assembled in external magnetic field. (b) Transmission electron microscope (TEM) images of the linear filaments at low and high (inset) magnifications. Due to the large difference in the electron density, the images exclusively show the distribution of the nanoparticles in the filaments and fatty acid remains invisible. (c) Change in the filament diameter along its contour (similar to the one visualized in (b)). (d-f) COMSOL^{TM} simulation snapshots of the nanoparticle chain growth in external magnetic field (horizontal). The color gradient represent the normalized magnetic field intensity in $\times 10^3$ A/m. Magnetic dipole-dipole attraction drives the directional assembly of the filaments as the high magnetic field intensity at the tip preferentially attracts the nanoparticles via magnetophoretic interactions.

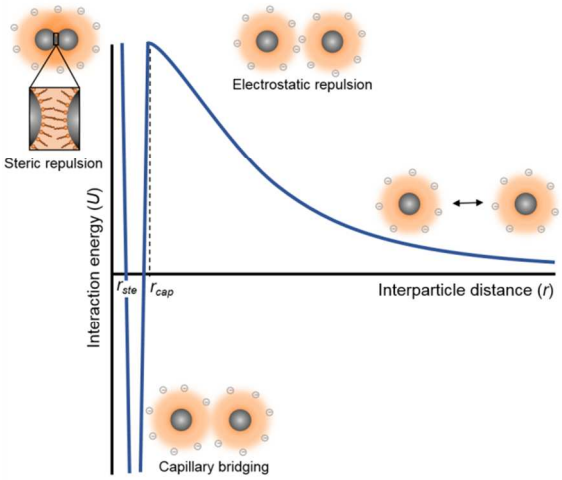

Figure 3. Sketch of the expected particle pair interaction energy of fatty-acid-coated iron oxide nanoparticles. The initial increase in energy (long-range repulsion) of two approaching particles can be caused by the repulsions between the negatively charged -COO^- groups of the fatty acid shell condensed around the nanoparticles. The instantaneous decrease in the energy at $r_{ste} < r < r_{cap}$ (strong attraction) is a result of the formation of fluid capillary bridge between the nanoparticles. The increase in energy at $r < r_{ste}$ corresponds to the steric repulsions between the C-chains of the fatty acid molecules adsorbed directly at the iron oxide surface (left inset).

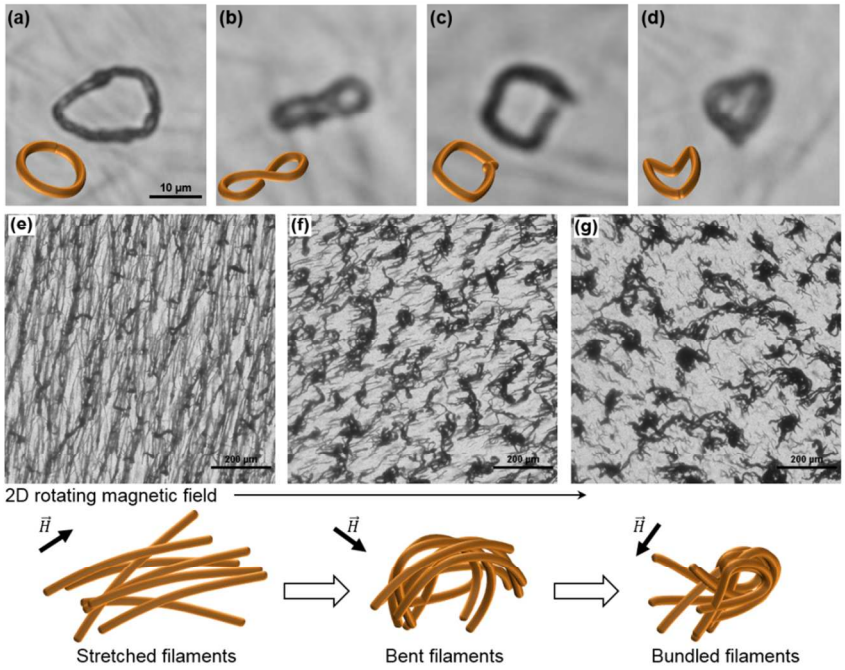

Figure 4. (a-d) Micrographs illustrating the reassembly of linear filaments into ring, square, "infinity" and heart-like unusual structures. The reassembly of filaments into closed loops was induced by instantaneous reversal of magnetic field polarizibility. The ring and infinity filament shapes were attained via curling by cis- and trans- pathways respectively (for details see text). (e-g) Microscope snapshots of the percolated multi-filament network in 2D rotating magnetic field. The filaments first attain partially bent and then bundled configurations in the rotating magnetic field.